Journal of Engineering and Applied Research (JEAR)

National University of Skills

Winter & Spring 2025, Vol. 2, No. 1, p. 139-158

Journal Homepage: https://jear.tvu.ac.ir

: 10.48301/jear.2025.515176.1107

Optimal Energy Management in Connected Microgrid Based on the Radial Basis Function Load Forecasting

Mostafa Jafari Kermani Pour [1], Farzin Fardinfar[2*], Mitra Mirhosseini[3]

[1]Department of Electrical Engineering, National University of Skills (NUS), Tehran, Iran

[2,3] Department of Electrical Engineering, Shahid Bahounar University, Kerman, Iran

ARTICLE INFO

Article Type:
Original Research

Received: 04.14.2025
Revised: 05.12.2025
Accepted: 07.16.2025

Keyword:
Microgrid-Connected
Energy Management
Demand Response
Radial Basis Function
Distributed storage

***Corresponding Author:**
Farzin Fardinfar
Email: *f.fardinfar@eng.uk.ir*

ABSTRACT

Due to their distinctive characteristics, such as flexibility and sustainable energy production, the use of renewable energy sources has significantly increased in recent years. Energy management systems are crucial to the efficient operation of prosumers. By selecting and incorporating the appropriate renewable energy sources, future grids' energy efficiency and operational stability can be significantly increased. The main objective of this research is optimal management of a Microgrid connected to the grid, which is considering the constraints and cost per hour, and the amount of production and consumption amounts are expressed. Microgrid-connected hybrid system model for the current research has been created using the available renewable energy sources. The energy management system incorporates a load prediction module and to improve this prediction, Radial Basis Function (RBF) is applied using artificial neural network. Furthermore, including the depreciation cost of renewable energy sources in the objective function, improves the daily operation cost of the loads. The system is optimized using the multi-objective particle swarm optimization algorithm, and the case study is considered as a real area in Kerman Province, Iran, with residential, industrial, and commercial loads. The case study results indicate a notable enhancement in in power losse reduction, achieved through optimal operational cost management following load forecasting using the RBF neural network approach.

E-ISSN: 3060-6357

Introduction

The number of microgrids (MGs) in the distribution network has recently increased due to the quick growth of smart grids (SG) and the Energy Internet. Each MG only considers the maximization of its own interests when producing and using power, neglecting the interests of the entire economy [1,2]. MGs are distributed power systems that utilize renewable energy resources (RERs) and electricity end users, possibly with controllable elastic loads [3]. Depending on where they come from, RERs can come from distributed storage (DS) or distributed generation (DG). Small-scale power generators that fall under the DG category include RER are such as wind turbines (WT) or photovoltaic (PV) generation. Distribution networks with residential or commercial end users, in rural or metropolitan regions, may be a component of MGs' functioning in either grid-connected or island mode [4]. In its consideration of efficient energy management for MGs, it takes into account economic dispatch, unit commitment, and demand-side control. Both grid-connected or standalone power generation modes for MGs are possible in a SG environment.

Most of the MG power is generated by RERs with intermittent bases. The RER's power generation and the erratic nature of load demands are both successfully managed by the MG central control system, which oversees and controls all MG unit operations. Ideal MG operations in an SG environment can help realize a number of benefits, including increased reliability, increased operation flexibility, peak shaving, lower energy costs, load balancing, auto control operation, protection, integrated energy management side (EMS) operation, matching load-generation capacity, minimal pollution, and improved power [5,6].

The conventional single MG merely uses medium-voltage lines to transport power to the distribution network, but modern energy systems are developing into complex interconnected systems without a clear distinction between energy "producers" and "consumers" [7]. The planning of the future SG gives top priority to the demand side's continued enthusiastic participation in energy management and trading initiatives as well as the successful integration of flexible loads (FLs), prosumers, and RERs into the energy system. Demand response programs (DRPs) can be used by MGs to balance system loads thanks to the inclusion of FLs. Peak shaving and peak load shifting may also be made possible by some energy management techniques, like DRPs, which could assist MGs in making better use of electricity [8]. When presenting a stochastic energy procurement problem for large electricity consumers, took into account the effects of DRPs on the system's operational costs [9]. Due to the fact that energy consumption shifts from expensive periods to inexpensive ones, Alemi [10] showed that DRPs could lower

the anticipated system operating costs. In [11], a new method for MG's DRP-based optimal operation is developed using three new hybrid machine learning-based techniques: the adaptive neuro-fuzzy inference system (ANFIS), the multilayer perceptron (MLP) artificial neural network (ANN), and the radial basis function (RBF) ANN. The specific projected load and weather information are taken into account by the proposed optimization approach.

One of the many crucial aspects of organizing, scheduling, dispatching, and managing power system operations is the precision of predictions of short- and long-term electric loads [12]. A few of the challenges utilities must overcome to develop forecasting methods include the enormous amounts of data provided by smart meters, the difficulty in identifying and quantifying the proper drivers of energy demand, and the requirement to avoid model over-fitting, particularly during peak demand. Other challenges result from the need to comprehend how various scenarios electricity consumption is affected by elements like temperature, humidity, the generation of renewable energy, and demand response participation. Here, we concentrate on short-term load forecasting, whose time horizon typically ranges from one hour to one week [13, 14]. Radial Basis Function (RBF) networks, a fascinating alternative to sigmoidal-type networks, are trained by a variety of machine learning algorithms and the effectiveness of Support Vector Regression (SVR) [15–16], ELM-Extreme Learning Machines [17–19], Decay RBF Neural Networks (DRNN) [18–19], and Error Correction (ErrCo) [19] have been examined in recent years.

This paper works on a grid-connected MG, which total loads are predicted by RBF network and the results of RBF are applied to calculate the load flow and optimization. The proposed integrated optimization, which is used by Multi-Objective Particle Swarm Optimization (MO-PSO) algorithm, finds the best value of RERs, DS, DGs and DRP. The case studies a real area in Kerman province located in southeastern part of Iran.

The remainder of the paper is organized as follows: Section 2 discusses the MG system's architecture and models the RERs including WT, PV, DS, and diesel-generator (D-G). Problem formulation is explained in Section 3, which includes DGs, DS, DR, RBF problems, and objective function. Section 4 highlights the test cases that are being under examination. The results and the simulation with (RBF, MO-PSO) tariffs are presented in Section 5 along with the simulation data for the study system. Finally, the conclusions are summarized in Section 6**.**

The Architecture of MG

Interactions of prosumer and EMS demonstrated in Fig.1 shows conceptual breakdown of the MG, which includes RESs like PV, WT, and DG units and the prosumers. DS has also been used in the architecture of the system for financial and reliability reasons. The internal unit of each MG is governed and controlled by an energy management center, which can also communicate with the higher-level grid to exchange information and energy or work in tandem with nearby MGs to coordinate and provide support.

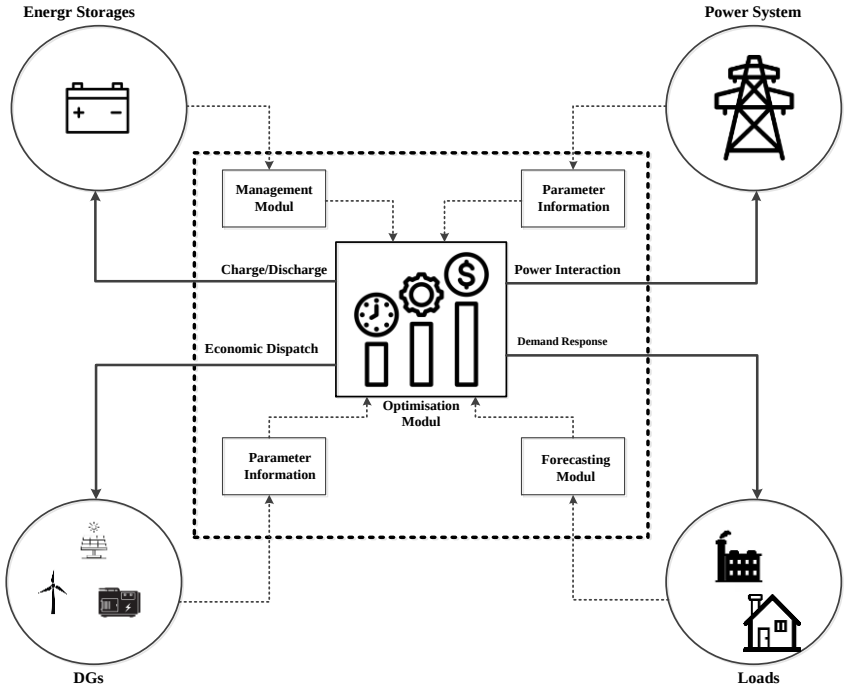

Figure 1. EMS configuration

The more precise way to describe MGs is as follows: prosumers typically pay for a specific contracted amount of power. Consumers want to use the electrical energy produced by prosumers since it is less expensive than what utilities offer. Because of this, the transfer of this form of energy between prosumers and consumers is considered an economic activity. It is crucial to remember that the prosumer gains from using less imported electricity during the specified times.

Methodology and Modeling

Power Generation Modeling of PV and WT

RER such as PV and WT are ideal for microgrids due to their abundance and sustainability. However, their output power depends heavily on environmental factors like solar irradiance, temperature, and wind speed, which must be accurately modeled. Here, real power generation of PV is given by [22]:

$$P_{pv}(t)=\left[P_{pv,stc}.\frac{G_T(t)}{1000}.\left[1-\gamma_m(T_j-25)\right]\right].N_{pv_s}.N_{pv_p} \qquad (1)$$

where *Ppv(t)* is the power generated by the PV module, *Ppv,stc* is the maximum generated power under standard conditions, *Gt(t)* is the value of standard irradiance, γ_m is the temperature coefficient in maximum power generation, *Tj* is PV cell temperature, and Npv_s and Npv_p are the number of series and parallel modules. T_j determines by:

$$T_j=T_{amp}+\frac{G_T}{G_{T,stc}}\times(NOCT-20) \qquad (2)$$

Where *NOTC* is cell temperature in a module when ambient is 20°C, solar irradiation is 0.8 kW/m^2, and wind speed is 1 m/s. The module efficiency, or η_t^{pv}, in equation (3) should be taken into account when calculating the output power of PV units.

$$\eta_t^{pv}=\eta_{rated}\left[1-\alpha(T_t+G_t\times\frac{NOCT-20}{800}-T_{ref})\right] \qquad (3)$$

Where η_{rated} and α are the temperature coefficient for cell efficiency and rated efficiency of PV measured at referenced temperature (0.004/◦C), respectively and T_{ref} is reference temperature (25◦C).

When calculating the output power of WT, environmental variables like surface area, air density, aerodynamic coefficient and wind speed- are considered to be essential components. When the wind speed is below or above the permissible speed, the wind turbine is forced to stop which is defined as cut-in and cut-out speed, respectively; which are states 1 and 4 in (4). Recent studies have presented the following approach, as an accurate solution [23].

$$P_w(t)=\begin{cases}0; & \upsilon(t)\le\upsilon_{c-i}\\ \left\{A+B\,\upsilon(t)+C\,\upsilon^2(t)\right\}\times P_{wt}; & \upsilon_{c-i}\le\upsilon(t)\le\upsilon_{wr}\\ P_{wt}; & \upsilon_{wr}\le\upsilon(t)\le\upsilon_{c-o}\\ 0; & \upsilon_{c-o}\le\upsilon(t)\end{cases} \qquad (4)$$

Here $P_w(t)$ is the output power of WT and $\upsilon(t)$, $\upsilon_{c\text{-}i}$, $\upsilon_{c\text{-}o}$, and υ_{wr} are wind speed, cut-in speed, cut-out speed, and nominal rated wind speed, respectively. *A*, *B,* and *C* are also wind power constants, which depend on type and scale of turbine.

DS System

The generation of PV or WT might not always be sufficient to meet the hourly energy demand, so it is important to have a sufficient amount of storage to handle this issue. As more electricity is generated from renewable sources than is needed during the charging process, there is excess generation available that can be stored in DSs. All of the DSs are viewed as batteries in this paper, and their charging state capacity can be calculated as:

$$E_{BAT}(t) = (1-\gamma) \times E_{BAT}(t-1) + \eta_{CH} \times \left[E_{UT}(t) + \sum_{n=1}^{m} E_{DGs}(t) \right] \quad (5)$$

Where $E_{BAT}(t)$ denotes battery storage in kWh; γ denotes the hourly self-discharging rate of battery; $E_{DGs}(t)$ and $E_{UT}(t)$ are excess DG generation and utility energy, respectively; and η_{CH} denotes the efficiency of battery during charging. When the amount of energy generated from renewable sources is lower than the amount of energy required to feed the demand and the cost of utility energy is high as well, the energy stored in the battery will be used to meet the demand. The following formula can be used to determine a battery's capacity while it is being discharged:

$$E_{BAT}(t) = (1-\gamma) \times E_{BAT}(t-1) - \frac{E_{\mathrm{Req}}(t)}{\eta_{DCH} \times \eta_{INV}} \quad (6)$$

Where:

$$E_{\mathrm{Req}}(t) = E_{DEM}(t) - \left[E_{UT}(t) + \sum_{n=1}^{m} E_{DGs}(t) \right] \quad (7)$$

Here, η_{DCH} and η_{INV} stand for the battery discharge rate and the efficiency of the inverter, respectively. E_{Req}(t) denotes the amount of energy needed to meet the load that is not met by the DGs or the utility, and E_{DEM}(t) stands for the total energy demand in the MG.

Demand Response Program

An economic load model that depicts the changes in customer demand in response to changes in the price of electricity was developed in order to formulate customer participation in DRP. A customer incentive system is also included in the model.

Elasticity in this paper is explained as the demand sensitivity with respect to the price which is calculated by:

$$EL(i,j) = \frac{\rho_0(j)}{d_0(i)} . \frac{\partial d(i)}{\partial \rho(j)} \quad (8)$$

Here *EL(i, j)* is cross elasticity and $\rho_0(j)$, $d_0(i)$, $d(i)$ and $\rho(j)$ are initial electricity price in *jth* hour, initial demand value in *ith* hour, load demand in *ith* hour and spot electricity price in *jth* hour, respectively.

If the electricity price changes over time, the demand will react in one of the ways explained hereafter. Several loads (e.g lights) can only be turned on or off on a specific period time of the day. Because of this, such loads only show sensitivity during a single time period, which is known as "self-elasticity" and this value is always negative. On the other hand, it is possible to shift some consumption from peak to off-peak or low periods (e.g industrial loads). This type of behavior is characterized by "multi-period sensitivity," and it is evaluated using "cross-elasticity". This value is always positive.

According to the cross-elasticity definition with the linearity assumptions, multi-period elastic loads can be defined as follows:

$$\frac{\partial d(i)}{\partial \rho(j)}: \text{constant for } i, \qquad j = 1,2,3,\ldots 24 \quad (9)$$

The linear relationship between prices and demands implies as follows [10]:

$$d(i) = d_0(i)\left[\frac{EL(i)(\rho(i)-\rho_0(i))}{\rho_0(i)} + 1\right] \quad (10)$$

Eq.10 describes load demand in single-period.

$$d(i) = d_0(i) + \sum_{\substack{i=1 \\ i\neq j}}^{24}\left\{\begin{matrix} EL(i,j).\dfrac{d_0(i)}{\rho_0(j)} \\ \times\left[\rho(j)-\rho_0(j)\right] \end{matrix}\right\} \quad i = 1,2,3,\ldots 24 \quad (11)$$

So, based on (11) which describes the load demand in multi-period we have:

$$d(i) = d_0(i).\left\{1 + \sum_{\substack{j=1 \\ j\neq i}}^{24} EL(i,j).\frac{\rho(j)-\rho_0(j)}{\rho_0(j)}\right\} \quad (12)$$

Combining single-period and multi-period data will result in the following responsive load economic model:

$$d(i) = d_0(i).\left\{\begin{matrix} 1 + EL(i,j).\dfrac{\rho(i)-\rho_0(i)}{\rho_0(i)} \\ + \displaystyle\sum_{\substack{j=1 \\ j\neq i}}^{24} EL(i,j).\frac{\rho(j)-\rho_0(j)}{\rho_0(j)} \end{matrix}\right\} \quad (13)$$

The equation above illustrates how much should be consumed by the customer to get the best results over a 24-hour period.

Forecasting Load

In a few recent studies for load prediction, radial basis function (RBF) has been used [20, 21]. In this study, an RBF-based artificial neural network (ANN) is used to predict load. Conventional feed-forward neural networks have been replaced in recent years by RBF networks, which have a shallow design but good generalization abilities. Due to the nature of RBF units, which affect the input space only within their radiuses, the mutual interactions between RBF units are not as significant as in the case of conventional sigmoid-type neural networks [24].

Because each RBF unit typically only influences a smaller subset of input patterns than conventional sigmoidal neural networks, RBF networks interact less than sigmoidal neural networks do. As a result, the generalization properties of RBF networks are greatly enhanced. RBF networks may have multiple outputs, but they are frequently used in cases with only one output (Fig. 2). Each hidden unit h in the hidden layer, which is made up of RBF units, executes a nonlinear operation that is specified by the activation function below.

$$\varphi_h(\boldsymbol{\chi}_p) = \exp\left(-\frac{\left\|\mathbf{y}_{p,h} - \mathbf{C}_h\right\|^2}{\partial_h^{\,2}}\right) \quad (14)$$

Here, $\varphi_h(\boldsymbol{\varkappa}_p)$ is hidden unit h in the hidden layer, C_h is the vector describing where the RBF center of unit is located, and ∂_h is the radius of the RBF unit. In place of radiuses, it is customary to use a gamma parameter γ_h, also referred to as the impact factor, instead of radiuses ∂_h. The relationship is defined as:

$$\gamma_h = (\partial_h^{\,2})^{-1} \quad (15)$$

As a result, (14) is converted to (16) as follows:

$$\varphi_h(\boldsymbol{\chi}_p) = \exp\left(-\gamma_h \times \left\|\mathbf{y}_{p,h} - \mathbf{C}_h\right\|^2\right) \quad (16)$$

The weighted sum of the outputs from the RBF units serves as the output signal for pattern p:

$$O_p = \sum_{h=1}^{H} w_h, \varphi_h(\boldsymbol{\chi}_p) + w_0 \quad (17)$$

In this method there are many parameters which should be adjusted [23]:

-Inputs weights $u_{i,h}$, (i=1,2,…I and h=0,1,2,…H)

-Gamma parameter γ_h, (h=0, 1, 2,…H)

-Locations of RBF centers ci,h (i=1,2,…I and h=0,1,2,…H)

- Output weights w_h (h=0, 1, 2,…H)

There are already a large number of specific RBF training algorithms. The majority of these algorithms only change the output weights w_h because altering RBF unit parameters using gradient-based methods is much more difficult than altering conventional neurons with sigmoidal activation functions.

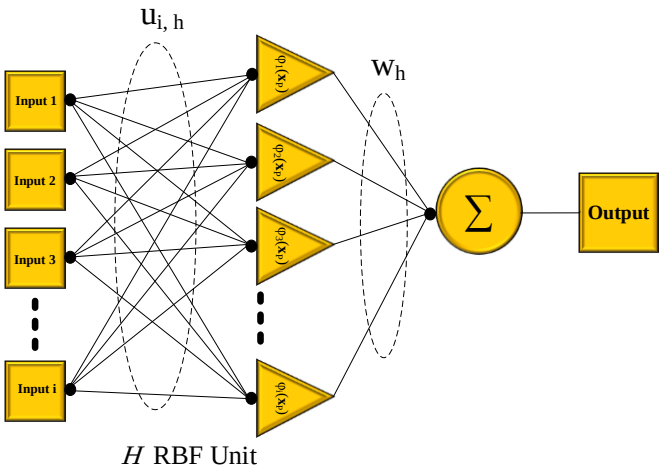

Figure 2. RBF network with I inputs, H hidden units and one output

Objective Function

Optimizing operational costs over the course of a 24-hour period is the primary goal of energy management for MGs. The cost function in MG is given by:

$$C_{total} = \sum_{t=1}^{24} \left[\begin{array}{l} \left(C_{DG}(t) + C_{DS}(t) + C_{DR}(t) + C_{grid}(t) \right) \\ +(P_{Loss}^{total} + Q_{Loss}^{total}) + VD \end{array} \right] \quad (18)$$

Here, The total operational cost C_{total} integrates both economic and technical objectives, combining generation costs, grid interaction expenses, and key power system performance indicators. Specifically, it includes the operational costs of distributed generation units $C_{DG}(t)$, demand response program participation $C_{DR}(t)$, distributed storage utilization $C_{DS}(t)$, and power exchange with the external grid $C_{grid}(t)$. To ensure system efficiency and stability, the objective function also accounts for total active and reactive power losses (P_{Loss}^{total} and Q_{Loss}^{total}) as well as the cumulative voltage deviation (VD) across all network buses. This unified formulation enables a balanced optimization of cost-effectiveness and power quality, minimizing financial expenditures while enhancing grid reliability and voltage profile.

All of parameters in objective function are standard normalized, which calculated by:

$$f_{in}(x) = \frac{f_i - f_{i,\min}}{f_{i,\max} - f_{i,\min}} \quad (19)$$

In (19) $f_{i,\min}$ and $f_{i,\max}$ are minimum and maximum of function f_i.

Operating Cost for Generation Units

The main DG units in a MG contain the D-G, PV, and WT. The operational cost of the D-G is a quadratic function, though the operational cost of WT and PV power is a simple linear function. They are expressed as follows:

$$\begin{aligned} C_{\infty} = & \sum_{N=1}^{N} (\alpha_{PV,i} \times \underbrace{P_{PV,i}(t) + \beta_{PV,i}}_{PV\ \mathrm{COST}}) \\ & + \sum_{M=1}^{M} (\alpha_{WT,i} \times \underbrace{P_{WT,i}(t) + \beta_{WT,i}}_{WT\ \mathrm{COST}}) \\ & + \sum_{K=1}^{K} (\alpha_{D-G,i} \times \underbrace{(P_{D-G,i}(t))^2 + \beta_{D-G,i} \times P_{D-G,i}(t) + \gamma_{D-G,i}}_{D-G\ \mathrm{COST}}) \end{aligned} \quad (20)$$

where N, M and K are the number of different distributed power sources; $\alpha_{PV,i}$ and $\beta_{PV,i}$ are the cost coefficients of PV; $\alpha_{WT,i}$ and $\beta_{WT,i}$ are the cost coefficients of WT; while $\alpha_{D\text{-}G,i}$, $\beta_{D\text{-}G,i}$ and $\gamma_{D\text{-}G,i}$ are the cost coefficients of D-G.

Operating Cost of DSs

The charging costs, discharge benefits, and switching costs for charging and discharging make up the majority of the DS unit's operating expenses. These expenses are defined as:

$$C_{DS,i}(T) = \sum_{t=1}^{T} (C_{CH,i}(t) - C_{DCH,i}(t)) + C_{switch,i}(T) \quad (21)$$

$$C_{CH,i}(t) = P_{CH,i}(t) \times \iota_{b-price} \quad (22)$$

$$C_{DCH,i}(t) = P_{DCH,i}(t) \times \eta_{DCH,i}(t) \times \iota_{b-price}(t) \quad (23)$$

$$C_{switch,i}(T) = (N_{CH,i}(T) + N_{DCH,i}(T)) \times \eta_{switch,i}(t) \quad (24)$$

Where $C_{switch,i}(T)$, $N_{CH,i}(T)$, $N_{DCH,i}(T)$ and $\iota_{b\text{-}price}(t)$ are the switch state cost, charge, discharge times and electricity base price at period T; $C_{CH,i}(t)$, $C_{DCH,i}(t)$ are the charging price and the discharging income at time t, respectively; $\eta_{DCH,i}(t)$ is the discharge rate.

Demand Response Cost

According to dispatchable circumstances, shifting, and operating costs, the loads in an MG are separated into critical load and flexible load categories. Their operation costs are determined by the actual load demand and related tariff rates. In the following:

$$C_{DR}(t) = -\sum_{i=1}^{N}\overbrace{(P_{crit,i}(t)\times\eta_{crit,i}(t))}^{\text{critical load}} + \sum_{i=1}^{M}\left[\overbrace{\begin{matrix}P_{flx,i}(t).(1-\lambda_{flx,i}(t)).\iota_{b-price}\\ +P_{flx,i}(t)\times\lambda_{flx,i}(t)\times\eta_{flx,i}(t)\end{matrix}}^{\text{flexible load}}\right] \quad (25)$$

$C_{crit}(t)$ and $C_{flex}(t)$ are the total operating costs of the critical and flexible load respectively; N and M are the number of corresponding loads; $P_{crit,i}(t)$, $P_{flx,i}(t)$ are the critical and flexible load demand respectively; $\eta_{crit,i}(t)$, $\eta_{flex,i}(t)$ are the critical load owing rate and the flexible load compensation rate, respectively[6].

Interaction Costs with External Distribution system

Purchase and sale are the two main components of the cost of interacting with the external distribution grid. The interaction cost between MG and external distribution system is defined as follows:

$$C_{grid} = \sum_{i=1}^{K}\left[\begin{matrix}(P^{buy}_{grid.i}(t)\times\eta^{buy}_{grid,i}\\ -P^{sell}_{grid.i}(t)\times\eta^{sell}_{grid,i})\times\iota_{b-price}\end{matrix}\right] \quad (26)$$

In (26), $P^{buy}_{grid.i}$ and $\eta^{buy}_{grid,i}$ are Purchased power and price factor for buying power also, $P^{sell}_{grid.i}$ and $\eta^{sell}_{grid,i}$ are power sold and sold factor for selling power, respectively.

Constraint

This section elaborates on the constraints considered in the MG modeling. The following equations represent the system constraints.

$$\sum_{\forall i,j\in\Omega_{Bus\,i,j}} P_{Gen} = \sum_{\forall i,j\in\Omega_{Bus\,i,j}} P_{Load} + \sum_{\forall i,j\in\Omega_{Bus\,i,j}} P_{Loss} \quad (27)$$

$$P^{grid}_{Gen} + P^{DG}_{Gen} + P^{DR}_{Gen} \pm P^{DS}_{Gen} = P_{Load} + P_{Loss} \quad (28)$$

$$\sum_{\forall i,j\in\Omega_{Bus\,i,j}} Q_{Gen} = \sum_{\forall i,j\in\Omega_{Bus\,i,j}} Q_{Load} + \sum_{\forall i,j\in\Omega_{Bus\,i,j}} Q_{Loss} \quad (29)$$

$$Q_{Gen}^{grid} + Q_{Gen}^{DG} + Q_{Gen}^{DR} = Q_{Load} + Q_{Loss} \quad (30)$$

$$V^{\min} \le V_i \le V^{\max} \qquad \forall i \in \Omega_n \quad (31)$$

$$V_{ESS}^{\min} \le V_{ESS} \le V_{ESS}^{\max} \qquad \forall i \in \Omega_n \quad (32)$$

$$i_i \le i^{\max} \qquad \forall i \in \Omega_n \quad (33)$$

Equations (27) to (30) represent the power balance constraints in the network, ensuring that the total power generation equals the sum of power consumption and losses. Equations (31), (32) define the voltage constraints, which regulate bus voltages, energy storage systems, and enforce upper/lower limits. Equation (33) specifies the permissible current flow limit in MG lines, which must always remain below its rated capacity.

Case Study

This study forecasts for solar irradiance, temperature, wind speed, and load are based on actual data that were gathered from a local meteorological station in the Kerman, Iran. The rates differ from one region to another due to the diverse climates. The city of Kerman (30245010" N, 57162402" E) has hot and dry summer weather, and is located in tropical region 2. Figure.3 displays the location of the test system. Figure.4 displays the solar irradiance, which the maximum of value occurs between 11 AM and 13 PM in a test day, and temperature of test system is shown in Figure.5. Figure.6 depicts the wind speed, in which Cut-in, cut-out, and average rated wind speeds are taken to be 4, 25, and 8.64 m/s in this paper. Figure.7 shows the percentage of various load sectors, i.e. Total demand for the MG is split between residential, commercial, industrial, agricultural, and public sectors.

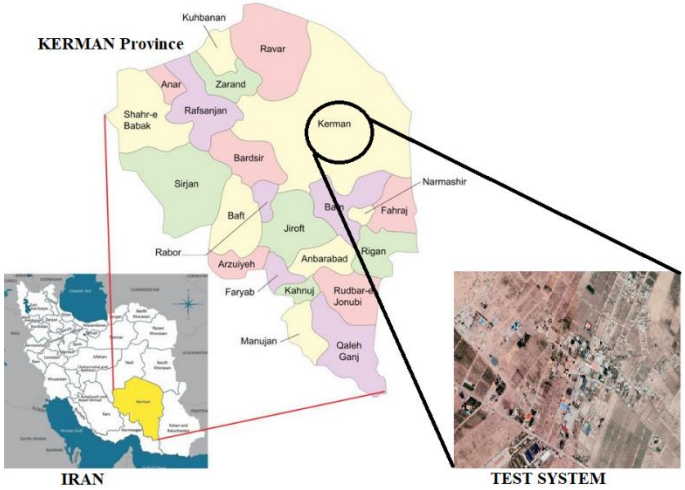

Figure 3. Geographical position of selected site

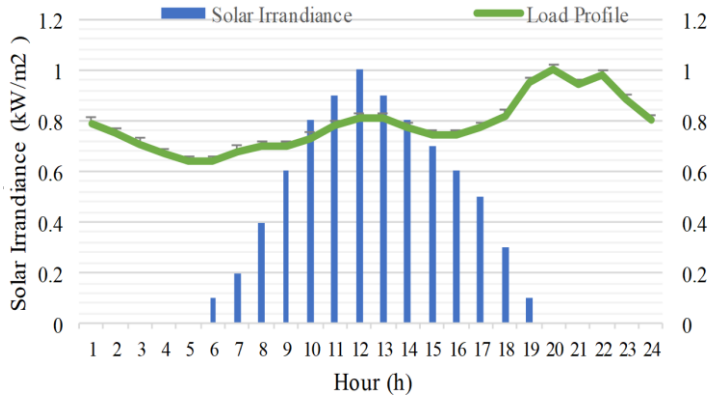

Figure 4. Solar irradiation of test day

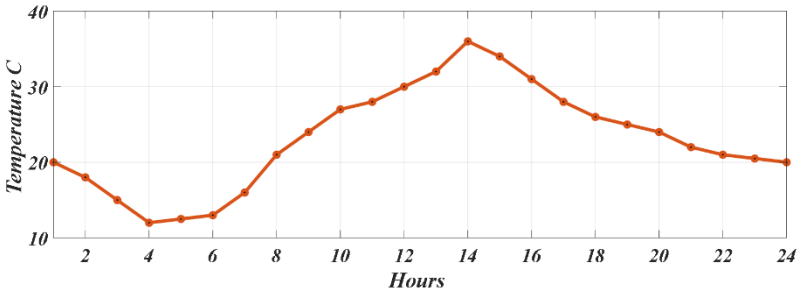

Figure 5. Temperature of test day

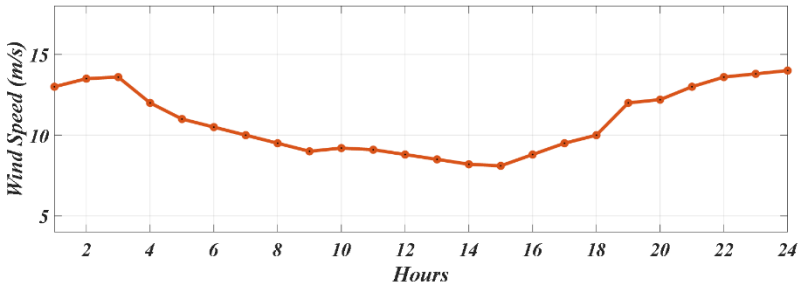

Figure 6. Wind speed of test day

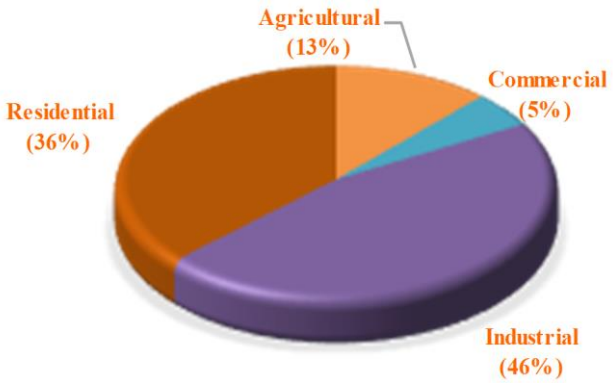

Figure 7. Different load types of MG

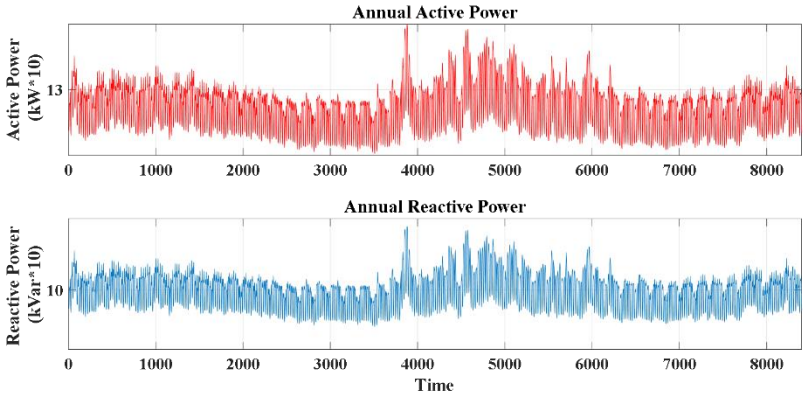

Figure 8. Annual Active and Reactive power

Figure. 8 illustrates the annual active and reactive power consumption profile by the microgrid load throughout the year.

Simulation, Result, and Discussion

Load forecasting

Short-term load forecasting is simulated by RBF method. Here, Figure. 9 shows real and predicted load and figure.10 shows an error histogram results for predicted load parameters. Based on the results, it was clear that predicted values for daily load are sufficiently accurate. The best validation performance for load forecasting in this paper is 2.5082e-06 at epoch 124 and figure.12 shows the corresponding results.

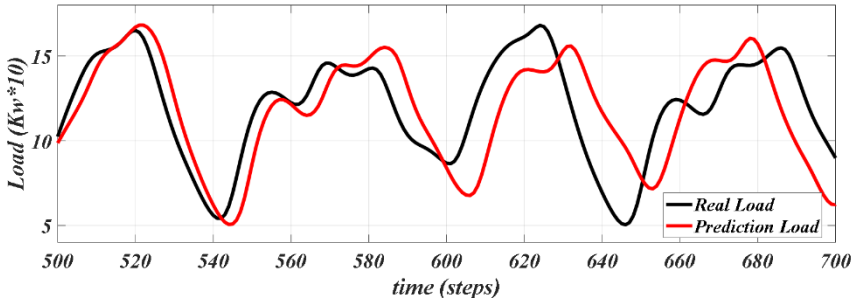

Figure 9. Real and predicted data of total load

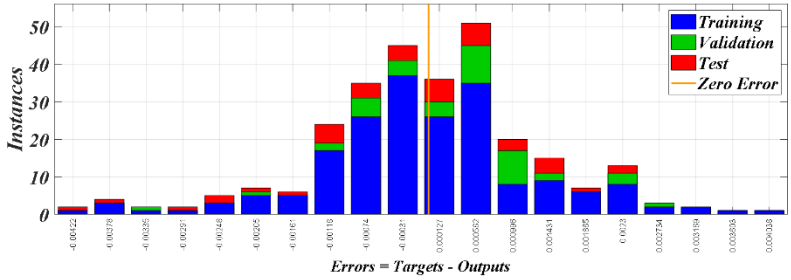

Figure 10. Error histograms for predicted load

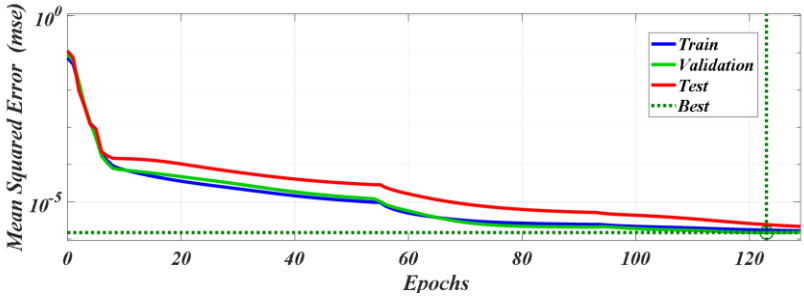

Figure 11. Validation Performance

EMS and Optimization

In this paper, to find the best value of DGs and DS in each hour, the multi-objective particle swarm optimization MO-PSO is used. Figure.11 shows load demand before and after demand response program. The simulation has been performed, and the results are given in Figure.13. This figure shows the best optimization of MG hourly which EMS determines DRPs and electrical interactions between MG and distribution grid. In addition, in Figure. 14 iterations of MO-PSO is shown where after 30 iterations, the best fitness value is obtained. As one can see from Figure. 15 and Figure. 16, active and reactive loss have been improved after applying the optimization technique.

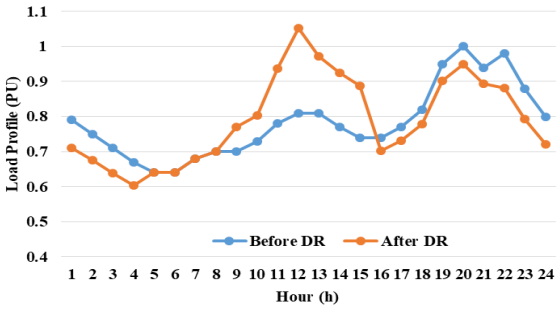

Figure 12. Load demand before and after EMS

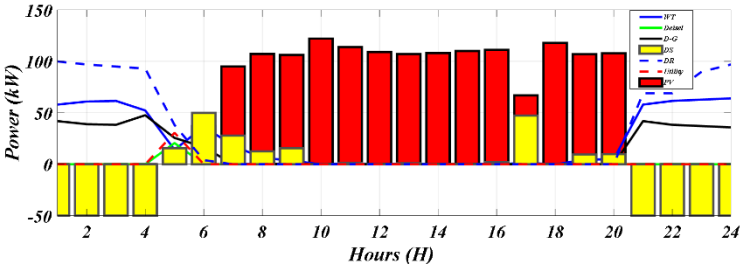

Figure 13. Integration of EMS in MG

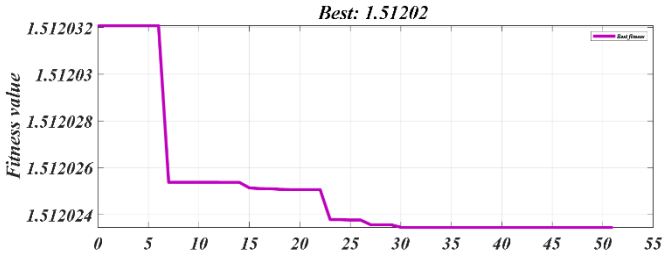

Figure 14. The best fitness

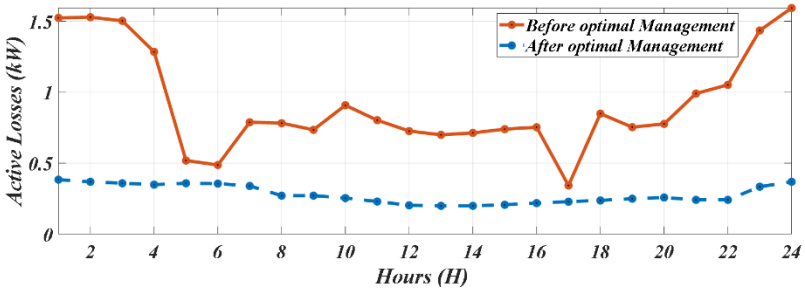

Figure 15. Total Active Loss

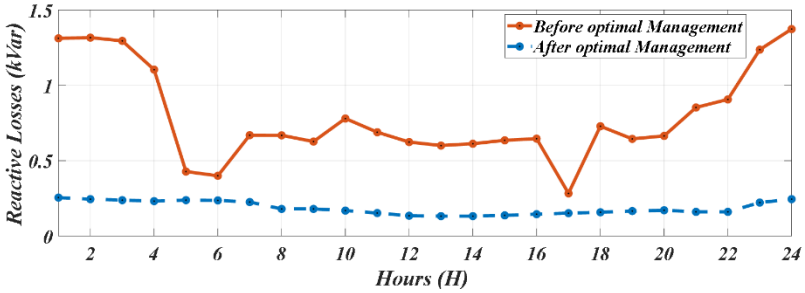

Figure 16. Total Reactive Loss

Conclusion

In this paper, the load forecasting has been simulated with RBF and a day-ahead optimization ESSs for a grid-connected MG has been introduced. With the aid of demand response initiatives, the current research has been concentrated on the creation of a MG renewable energy system. In this work, with the appropriate energy management, the interaction between generation and consumption as well as MG have been proved to be in the best condition where total losses and voltage deviation were minimized. Moreover, DS and DRP reduced the total cost of MG and grid dependence on power distribution network have also been estimated. MO-PSO is used for optimization of MG operation models. The results of the overall analysis reveals that the suggested MG planning and operation modeling approach could provide good solutions while maximizing distributed generations and distributed storage integration with the help of DRPs. As evident from the results, the microgrid demonstrated significantly improved performance after optimization, with remarkable enhancement in power loss reduction.The simulation results when applied on a real area in Kerman, Iran, verifies the suggested method.

References

[1]Arasteh, H., Vahidinasab, V., Sepasian, M. S., & Aghaei, J. (2018). Stochastic system of systems architecture for adaptive expansion of smart distribution grids. *IEEE*

Transactions on Industrial Informatics, *15*(1), 377-389. https://doi.org/10.1109/TII.2018.2808268

[2]Chen, F., Liu, J., Zhao, M., & Liu, H. (2022). Congestion identification and expansion planning methods of transmission system considering wind power and TCSC. *IEEE Access*, *10*, 89915-89923. https://doi.org/10.1109/ACCESS.2022.3201892

[3]Mofidian, R., Hassankhani, I., Jahanshahi, M., Hosseini, S. S., & Miansari, M. (2024). Cost Effective Design of a 200 kW On-grid Rooftop Photovoltaic System Using PVsyst Software in Shiraz. *Journal of Engineering and Applied Research*, *1*(1), 13-24. https://doi.org/10.48301/jear.2024.194109

[4]Liu, X., Zhao, T., Deng, H., Wang, P., Liu, J., & Blaabjerg, F. (2022). Microgrid energy management with energy storage systems: A review. *CSEE Journal of Power and Energy Systems*, *9*(2), 483-504. https://doi.org/10.17775/CSEEJPES.2022.04290

[5]Zhao, Z., Guo, J., Luo, X., Lai, C. S., Yang, P., Lai, L. L., Li, P., Guerrero, J. M., & Shahidehpour, M. (2022). Distributed robust model predictive control-based energy management strategy for islanded multi-microgrids considering uncertainty. *IEEE Transactions on Smart Grid*, *13*(3), 2107-2120. https://doi.org/10.1109/TSG.2022.3147370

[6]Gao, Y., & Ai, Q. (2021). Demand-side response strategy of multi-microgrids based on an improved co-evolution algorithm. *CSEE Journal of Power and Energy Systems*, *7*(5), 903-910. https://doi.org/10.17775/CSEEJPES.2020.06150

[7]Xu, H., Meng, Z., Zhao, R., Wang, Y., & Yan, Q. (2020). Optimal dispatching strategy of an electric-thermal-gas coupling microgrid considering consumer satisfaction. *IEEE Access*, *8*, 173169-173176. https://doi.org/10.1109/ACCESS.2020.3024931

[8]Achour, Y., Ouammi, A., & Zejli, D. (2021). Model predictive control based demand response scheme for peak demand reduction in a Smart Campus Integrated Microgrid. *IEEE Access*, *9*, 162765-162778. https://doi.org/10.1109/ACCESS.2021.3132895

[9]Abdollahi, A., Moghaddam, M. P., Rashidinejad, M., & Sheikh-El-Eslami, M. K. (2011). Investigation of economic and environmental-driven demand response measures incorporating UC. *IEEE Transactions on Smart Grid*, *3*(1), 12-25. https://doi.org/10.1109/TSG.2011.2172996

[10]Aalami, H., Moghaddam, M. P., & Yousefi, G. (2010). Demand response modeling considering interruptible/curtailable loads and capacity market programs. *Applied energy*, *87*(1), 243-250. https://doi.org/10.1016/j.apenergy.2009.05.041

[11]Zhang, Y., & Song, X. (2019). Load prediction of space deployable structure based on FBG and LSTM. *IEEE Access*, *7*, 13715-13722. https://doi.org/10.1109/ACCESS.2019.2893364

[12]Chen, B., Huang, D., Su, Q., Huang, T., Ling, F., & Liu, Z. (2020). Hierarchical Evaluation of Distribution Network Access Capacity Taking Into Various Prosumer Group

Load Forecasts. *IEEE Access*, *8*, 179901-179908. https://doi.org/10.1109/ACCESS.2020.3026549

[13]Razavi, S. E., Arefi, A., Ledwich, G., Nourbakhsh, G., Smith, D. B., & Minakshi, M. (2020). From load to net energy forecasting: Short-term residential forecasting for the blend of load and PV behind the meter. *IEEE Access*, *8*, 224343-224353. https://doi.org/10.1109/ACCESS.2020.3044307

[14]Kim, K.-H., Youn, H.-S., & Kang, Y.-C. (2000). Short-term load forecasting for special days in anomalous load conditions using neural networks and fuzzy inference method. *IEEE Transactions on Power Systems*, *15*(2), 559-565. https://doi.org/10.1109/59.867141

[15]Taghandiki, K. (2024). Quantum Machine Learning Unveiled: A Comprehensive Review. *Journal of Engineering and Applied Research*, *1*(2), 29-48. https://doi.org/10.48301/jear.2024.446673.1021

[16]Karayiannis, N. B., & Xiong, Y. (2006). Training reformulated radial basis function neural networks capable of identifying uncertainty in data classification. *IEEE Transactions on Neural Networks*, *17*(5), 1222-1234. https://doi.org/10.1109/TNN.2006.877538

[17]Cao, J., Zhang, K., Yong, H., Lai, X., Chen, B., & Lin, Z. (2018). Extreme learning machine with affine transformation inputs in an activation function. *IEEE transactions on neural networks and learning systems*, *30*(7), 2093-2107. https://doi.org/10.1109/TNNLS.2018.2877468

[18]Hou, M., & Han, X. (2010). Constructive approximation to multivariate function by decay RBF neural network. *IEEE Transactions on Neural Networks*, *21*(9), 1517-1523. https://doi.org/10.1109/TNN.2010.2055888

[19]Tan, P.-L., Cheah, C.-L., & Ho, C.-K. (2014). Hardware implementation of Reed-Solomon error correction technique for wireless sensor network based on error pattern analysis. 2014 IEEE Region 10 Symposium. https://doi.org/10.1109/TENCONSpring.2014.6863055

[20]Dongxiao, N., Ling, J., & Jie, T. (2011). Improved RBF network applied to short-term load forecasting. 2011 IEEE 2nd International Conference on Software Engineering and Service Science. https://doi.org/10.1109/ICSESS.2011.5982477

[21]Aoyang, H., Shengqi, Z., Xuehui, J., & Zhisheng, Z. (2021). Short-term load forecasting model based on RBF neural network optimized by artificial bee colony algorithm. 2021 IEEE 2nd International Conference on Big Data, Artificial Intelligence and Internet of Things Engineering (ICBAIE). https://doi.org/10.1109/ICBAIE52039.2021.9390043

[22]Fardinfar, F., & Pour, M. J. K. (2023). Optimal placement of D-STATCOM and PV solar in distribution system using probabilistic load models. 2023 10th Iranian

Conference on Renewable Energy & Distributed Generation (ICREDG). https://doi.org/10.1109/ICREDG58341.2023.10091990

[23]Haseeb, M., Kazmi, S. A. A., Malik, M. M., Ali, S., Bukhari, S. B. A., & Shin, D. R. (2020). Multi objective based framework for energy management of smart micro-grid. *IEEE Access*, *8*, 220302-220319. https://doi.org/10.1109/ACCESS.2020.3041473

[24]Cecati, C., Kolbusz, J., Różycki, P., Siano, P., & Wilamowski, B. M. (2015). A novel RBF training algorithm for short-term electric load forecasting and comparative studies. *IEEE transactions on Industrial Electronics*, *62*(10), 6519-6529. https://doi.org/10.1109/TIE.2015.2424399